KES Transactions on Sustainable Design and Manufacturing I
Sustainable Design and Manufacturing 2014 : pp.120-135 : Paper sdm14-053

Is there a relationship between product shape complexity and process energy consumption in Electron Beam Melting?

M. Baumers, C. Tuck, R. Wildman, I. Ashcroft, and R. Hague

Additive Manufacturing and 3D Printing Research Group (3DPRG), Faculty of Engineering, University of Nottingham, Nottingham, NG7 2RD, UK
martin.baumers@nottingham.ac.uk

Abstract Additive Manufacturing (AM) technology is capable of building up component geometry in a layer-by layer process, entirely without tools, moulds or dies. One advantage of the approach is that it is capable of efficiently creating complex product geometry.
Using experimental data collected during the manufacture of a titanium test part on a variant of AM technology, Electron Beam Melting (EBM), this research studies the effect of a variation in product shape complexity on process energy consumption. This is done by computationally measuring quantifiable characteristics associated with shape complexity (based on the concept of convexity) and correlating these to process energy consumption on the EBM system. Only a weak correlation is found between the complexity metric and energy consumption (ρ=0.35), suggesting that process energy consumption is indeed not driven by shape complexity.
This is discussed in the context of the energy consumption of computer-controlled machining technology, which forms an important substitute to EBM. This research concludes that EBM, as a variant of AM technology, provides a pathway to the energy efficient manufacture of highly functional products.

1. Introduction

Researchers argue that action is needed to limit anthropogenic climate change, it is claimed that humanity's ecological footprint already far exceeds earth's capacity [1,2]. Moreover, an understanding of the emissions associated with manufacturing processes is essential regarding decision making towards sustainability. In particular, the measurement of carbon emissions, known as 'carbon accounting', requires a fundamental understanding of the energy flows associated with production processes [3].

Additive Manufacturing (AM) is a relatively recent manufacturing approach, developed in the 1980s and 1990s [4]. The ASTM [5] defines AM processes as being capable of "joining materials to make objects from 3D model data, usually layer upon layer, as opposed to subtractive manufacturing methodologies". This paper assesses the energy consumption characteristics of one particular AM technology variant, Electron Beam Melting (EBM), which has been developed by the Swedish AM equipment manufacturer Arcam AB [6].

The general operating principle of EBM and the main system components are described in Figure 1. An electron beam is emitted from a beam column (a) and deflected to selectively melt the surface of a powder bed (b) layer by layer. After completing each layer, the build platform (c) moves down by an increment and the "powder rake" (d) deposits a fresh layer of metal powder, stored in powder hoppers (e). The wiper also discards any excess powder into overflow bins (f) for re-use. This cycle repeats until the build is complete. After completion of all layers, the build platform (c) holding the products is removed.

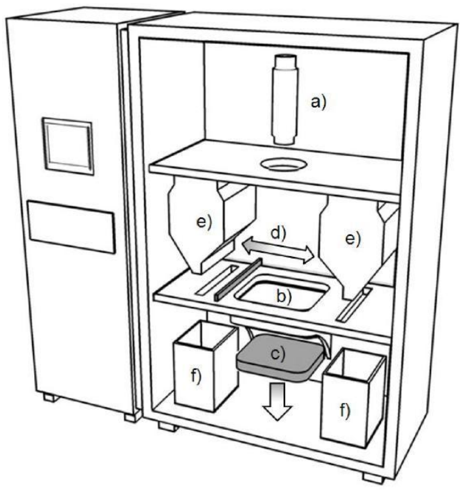

<u>Figure 1: Main components of an EBM system</u>

Image source: own work

For details on EBM's operating principle, see Hopkinson and Dickens [7], Heinl et al. [8], or Murr et al. [9]. EBM platforms have been judged to be particularly energy efficient variants of AM [8, 10, 11]. Strutt [12] points out that energy transfer by electron beam is around 10 times more efficient than by laser beam, which is employed by most other metallic AM technology variants. Table 1 summarises important characteristics of the investigated A1 EBM machine.

Table 1: Arcam A1 system characteristics, as employed for this research

System type	Arcam A1
Beam type	Electron beam
Maximum beam energy	3000 W
Nominal build volume size (X / Y / Z)	200 * 200 * 180 mm
Measured usable platform area (X / Y)	180 * 180 mm
Build material	Titanium, Ti-6Al-4V
Layer thickness	70 µm
Process atmosphere	Vacuum, with addition of He
Powder bed temperature	~700º C
Power supply	400V, 16A, multi-phase
Chiller on external power	no
Parts connected to base plate through supports	no
Manufacturer reference	Arcam AB [6]

It is suggested that AM technology has two main advantages over other manufacturing processes [13]. Firstly, AM allows the manufacture of designs without many of the geometric constraints that apply to other techniques. Secondly, AM enables the manufacture of customised products in small volumes at a relatively low average cost. The current state of AM technology, however, carries a set of generic process limitations [14], acting as a barrier to the adoption of AM process in some applications:

- limited material selection and characteristics,
- low process productivity,
- low dimensional accuracy,
- rough surface finish,
- repeatability and quality issues,
- relatively high unit cost at medium and large volumes.

In the production of small, geometrically complex or customised parts, EBM has been adopted in place of Computer Numerically Controlled (CNC) machining processes [15, 16]. There are striking differences between the additive operating principle of EBM and the subtractive method of CNC, which is, unlike EBM, a mature technology and has been adopted extensively [17]. This research identifies the impact on energy inputs resulting from these differences.

In the context of the estimation of production cost, it has been suggested that AM allows the manufacture of more complex product geometry at no additional (“marginal”) cost [18]. Presenting the results of a previous study of the energy inputs used by an EBM system during the production of specially designed test parts [19], this research presents an analysis correlating process energy consumption to characteristics associated with geometric complexity.

Being able to make the statement that energy is independent of the specifics of shape or geometry has interesting consequences. If shown to be true, the creation of elements of extra shape complexity would not require additional process energy consumption, allowing the provision of additional functionality at zero energy cost.

2. Methodology

To facilitate this investigation, it was decided to base power monitoring experiments on a standardised power monitoring geometry, as done by Mognol et al. [20]. The layer-by-layer operating principle of EBM allows the design of a power monitoring geometry tailored for the analysis of the impact of geometric variables on energy consumption by varying the part's cross section along the vertical ("Z") direction. The resulting test part, shown in Figure 2, exhibits a suitable variation in two parameters, shape complexity and cross-sectional area, as will be explored in the following sections.

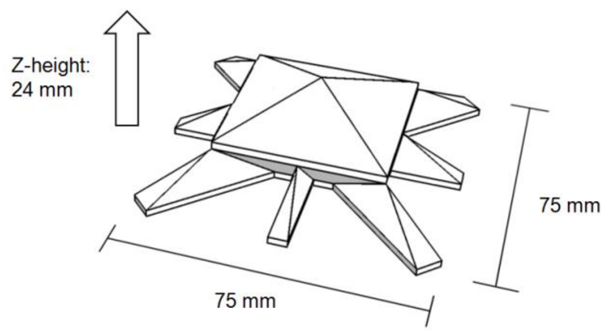

Figure 2: Standardised power monitoring geometry

Image source: Baumers [19]

The part's lower half is designed to assess the effect of shape complexity on energy inputs. This is done by changing a complex, star-shaped cross section with a square cut-out in the centre into a square cross section (at 12 mm Z-height). In the upper half of the geometry, the effect of cross-sectional area, reflective of overall part size, is explored. This is achieved by simply reducing cross section area A down to a value of zero, forming a single vertex in a pyramid-like upper tip. A further point of consideration in the design of the "spider" shape shown in Figure 1 was that some areas of the geometry feature negative wall angles. To avoid the use of support structures in the build experiments on the EBM system, the part was designed to not exceed negative wall angles of 45º.

2.1 Implementing a complexity measurement algorithm

An algorithmic approach developed by Psarra and Grajewski [21] associates the measurement of various metrics based on convexity with two-dimensional (2D) shape complexity. This technique was originally designed to computationally assess floor plans in architecture. In an adapted form, combined with an implementation inspired by radar systems, it allows the quantification of shape features associated with complexity in the test part shown in Figure 2 (and indeed any other part). In the context of this research it is particularly suitable as it is able to capture aspects associated with both the topological and geometrical aspects of complexity.

Transferring this technique to the analysis of three-dimensional (3D) solid geometry, the special layer-by-layer operating principle of AM allows the underlying 2D method to be maintained. This is possible because current additive equipment, such as the analysed EBM platform, operates in a strictly sequential manner completing each horizontal layer before depositing the next layer onto the existing geometry. Thus, AM permits a separate analysis of every 2D cross section.

By subjecting the cross section of a test part to a controlled variation along the test part's Z-axis, this research extends the original algorithmic approach [21]. Effectively, a continuous 3D solid is split into a sequence of 2D layers, so that the level of shape complexity can be varied within one build. The effect of the variation of shape complexity on process efficiency of AM can then be studied.

The first step towards the computational approach is of course a discretisation process. The complexity measurement algorithm is based on a manually discretised version of the test part shown in Figure 2, which is hard coded in a 3D array. Corresponding to the discretisation resolution in (1 mm)^3 volumetric pixels ("voxels"), the variation of shape complexity is measured in 1 mm intervals of Z-height. This resolution was chosen to balance the computational power needed for this approach (written in C++) with sufficient accuracy.

Once the specifically designed power monitoring geometry is discretised, the next step is to develop an algorithm that is designed to assess each discrete voxel element of the part's surface for complexity in a succession of horizontal cross sections (analogous to build layers). Expressed intuitively, the proportion of other surface elements that are directly visible from specific loci in a layer can thus be identified. The outcome of this calculation is a mean connectivity value (*MCV*) characterising the shape complexity of each horizontal slice of the test part. Mimicking the layer-by-layer principle of AM, the resulting algorithm assesses each layer separately, resulting in a series of *MCV* values for each horizontal layer of the discretised test geometry.

The actual algorithm underlying the measurement of such "visibility" is inspired by radar systems used to measure the distance of surrounding objects relative to a location. Radar systems operate by emitting signals in predetermined directions, often using antennae rotating around a Z-axis, as shown in Figure 3.

a) b)

Figure 3: Operating principle of radar
Image source: a) Baumers [19], (b) http://www.clker.com/clipart-43661.html

A Cartesian coordinate system is used in the implementation, which may deviate from the original inspiration. The principle of the measurement algorithm is very similar, however. Starting with the first element of the perimeter of first the layer under consideration, a 'radar signal' is emitted. Once the signal has been sent, it travels through the discretised voxel space in the predetermined direction. Where it strikes another element of the surface, the location is recorded. If it does not strike the perimeter at any location, for example if it is emitted towards the outside of the shape, no impact location is registered.

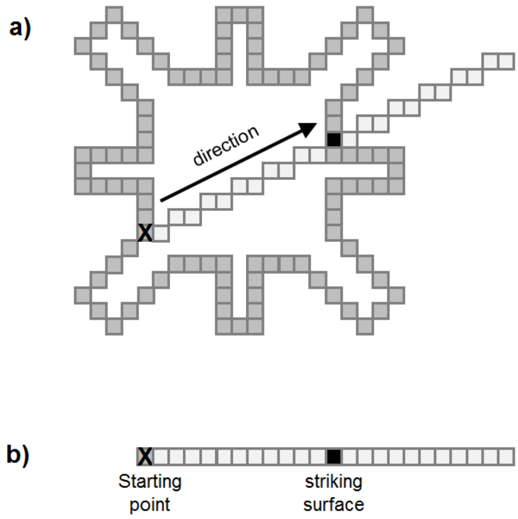

Figure 4: Implementation of occlusion measurement

Image source: Baumers [19]

This radar-inspired implementation works as follows: as illustrated in Figure 4a, the algorithm reads discretised information on part geometry in a particular direction, recording the content of the voxels cells approximating the part in a one-dimensional array (Figure 4b). In this sequence, beginning from the starting point, each entry is interrogated for a surface hit. The location of the first cell struck in this sequence is then recorded in a further array.

The direction, or gradient, of the 'radar beam' is then changed by one increment in counter clockwise direction (as illustrated in Figure 3b) and new information is read into the one dimensional array (Figure 4b). This is repeated in a loop, until the full 360º circle is complete around the starting point and all visible cells have been recorded. In the following step, the algorithm compares the location of the recorded visible elements to what should be visible without occlusion.

If every existing surface element is visible, the shape is deemed fully convex, as proposed by Psarra and Grajewski [21]. For intermediate results, a value of connectivity $CV \in]0,1]$ will be the result. This procedure is repeated for all '*n*' elements of the perimeter in layer '*i*', enabling the calculation of the mean connectivity value MCV_i for each layer, where:

$$MCV_i = \frac{\sum_{n=1}^{n} CV_n}{n} \tag{1}$$

MCV is calculated for all layers in the discretised approximation of the test part. Effectively, MCV_i reflects shape complexity present in the '*i*'th horizontal cross section if the part and thus forms a measure of 2D shape complexity.

2.2 Power monitoring experiments

To assess the effect of a variation in part geometry on the energy consumed to deposit a layer, a build experiment was been performed on the Arcam A1 EBM system. Acknowledging that AM systems of this type only operate efficiently if the available build capacity is utilised [22], a batch of five power monitoring test parts was produced in a full build experiment. All test parts were built in the same orientation directly onto the removable build plate, without any connecting or support structures.

The electricity consumption during the build experiments was recorded using a Yokogawa CW240 digital multi-purpose power meter (Yokogawa Electric Corp., 2004); the main variable of interest being mean real power consumption across the three phases and the neutral line. To assemble the required dataset, it is necessary to synchronise the collected energy consumption data with the log files created by the A1's operating system, providing information on machine state and build progress. This information is extracted from the build log files in the *.plg file format using Arcam's LogStudio tool (v.3.1.51).

3. Results

Cross-sectional shape complexity is quantified by calculating a metric of shape complexity, which is the mean value of "visibility", MCV_i, for each layer '*i*', as shown in equation (1). As the implementation of the measurement algorithm is based on a resolution of (1 mm)^3 voxels, the corresponding variation of test part parameters is measured in 1 mm intervals of Z-height.
Figure 5 shows the variation of three parameters along the test part's Z-axis: the total area of the part's cross section, the cross-sectional perimeter length and the parameter of shape complexity. For exposition, *MCV* is shown in inverted form, such that a high value of MCV^{-1} indicates high cross-sectional shape complexity.

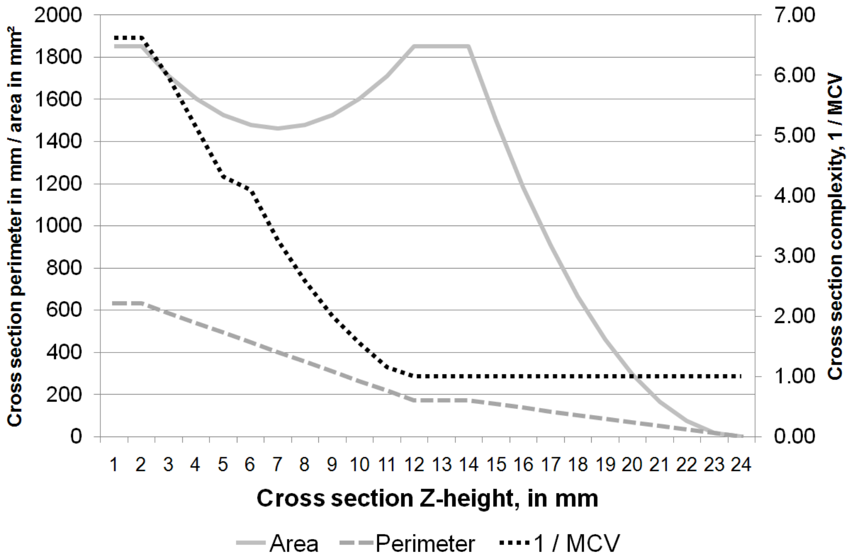

Figure 5: Variation of parameters of geometry
Image source: Baumers [19]

As Figure 5 demonstrates, the area of the cross-sections dips between 2 and 12 mm of Z-height, from an initial value of 1850 mm² to around 1450 mm². This fluctuation occurs alongside the controlled variation of *MCV*. The fact that both parameters are varied in parallel complicates the analysis of the pure effect of a variation of *MCV*. However, it does allow the design of a relatively simple polygonal test part without curved surfaces, as shown in Figure 2. The irregularity in the MCV^{-1} curve at a Z-height of 6 mm results from the use of a discretised voxel representation of part geometry. It is thus an artefact of the discretisation technique and should be ignored. Figure 5 further demonstrates that the design of a test part varying parameters of complexity and cross-sectional area is successful. The effect of the designed variation of area and complexity can be explored in conjunction with AM process energy consumption data.

2.2 Power monitoring results

Build operations on an EBM platform consist of four phases: system start-up, preheating, build phase and machine cool-down. For the full build and single part experiments, the energy consumption results are reported in Table 2, listing process time, mean real power consumption and cumulative energy consumption during the various phases of the build, resulting in a specific energy consumption of 59.96 MJ per kg deposited, which corresponds to the energy consumption results reported for other AM technology variants [23].

Table 2: EBM power monitoring results

	Full Build
Number of parts in build	5
Total build time	300 min
Warm up time: machine start-up	10 min
Warm up time: preheating	14 min
Build time	260 min
Cool-down time	17 min
Mean real power consumed	2.17 kW
Mean real power consumed: machine start-up	1.09 kW
Mean real power consumed: preheating	3.90 kW
Mean real power consumed: build	2.22 kW
Mean real power consumed: cool-down	0.60 kW
Total energy consumption	39.16 MJ
Energy consumption: machine start-up	0.62 MJ
Energy consumption: preheating	3.27 MJ
Energy consumption: build time	34.66 MJ
Energy consumption: cool- down	0.61 MJ
Energy consumed per part	7.83 MJ
Energy consumed per cm3	0.27 MJ
Specific energy consumption per kg deposited*	**59.96 MJ**

* assuming 100% part density, at 4.43 g/cm^3

By combining the energy consumption data with the information retrieved from the machine’s log file, it is possible to divide the energy invested during the core build time into three machine activities: i) layer preparation, ii) layer preheating and iii) melting.

Figure 6 shows that the energy expended during layer preparation (data loading and fresh powder deposition) fluctuates around a constant mean throughout the build (approximately 10 kJ per layer). In contrast, the energy expended during the preheating state exhibits a linear, slightly negative, trend – most likely due to a gradual warming up of the machine frame during the build process. More interestingly, the energy expended for the selective melting of the cross sections fluctuates strongly. The initial spike in energy consumption (during the first layer) is explained by repeat melting to ensure full attachment of parts to the build platform.

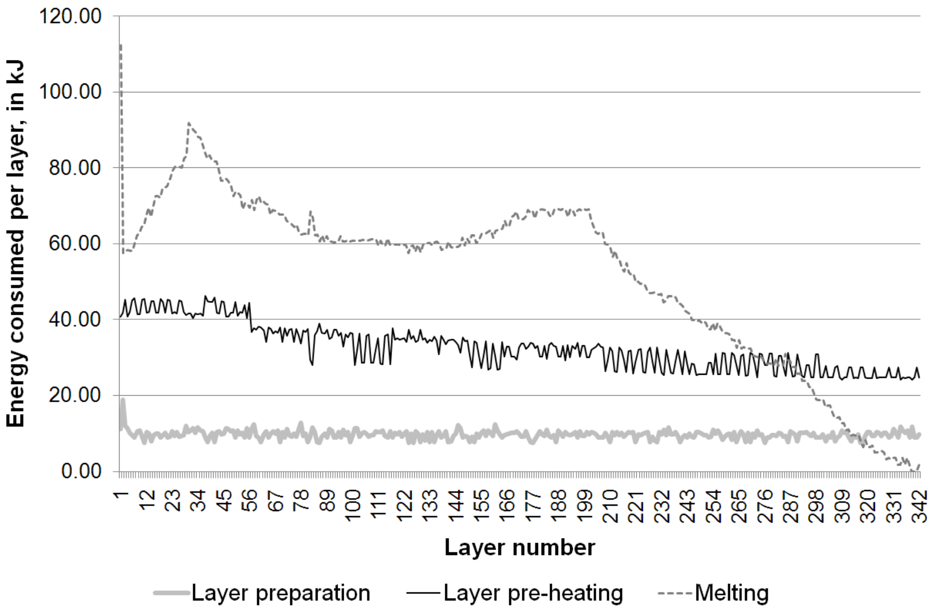

Figure 6: EBM energy invested per layer, by activity
Image source: Baumers [19]

3.2 Correlation between complexity and energy

Visual inspection of Figure 6 suggests that the observed pattern of energy expenditure for melting (dashed line) can be explained by cross-sectional area. The Pearson product-moment correlation coefficient $\rho_{X,Y}$,where

$$\rho_{X,Y} = \frac{cov(X,Y)}{\sigma_X \sigma_Y}, \tag{2}$$

and $\sigma_X \sigma_Y$ is the product of the standard deviations of variables X and Y, can be used to express the degree of linear dependence between two variables. A sample correlation coefficient $\rho_{Area,Layer\ Energy}$ = 0.9699 between selective melting energy and cross sectional area (in 1 mm intervals of Z-height) suggests that total melting energy consumption is indeed determined by cross sectional area, and thus by overall part mass.

Further applying correlation coefficients, the effects of various aspects of geometry on the energy expended for layer melting can be studied. Focussing on the portion of the build containing variation of shape complexity (1-12 mm Z-height, as shown in Figure 5), correlation coefficients between layer energy and cross-sectional perimeter length, complexity and melting area can be compared:

$$\rho_{Perimeter,Layer\ Energy} = 0.6568$$
$$\rho_{Area,Layer\ Energy} = 0.8263$$
$$\rho_{MCV,Layer\ Energy} = -0.3544$$

The coefficients demonstrate that melting energy consumption correlates strongly with cross section area (0.8263), and to a lesser extent with perimeter length (0.6568). The correlation coefficient between layer energy consumption and the used measure of shape complexity (-0.3544) is small. This can be viewed as evidence of a weak or potentially absent association between EBM energy consumption and cross-sectional shape complexity. It should be noted that the negative correlation coefficient originates from the formulation of MCV_i (a high value indicates a small degree of shape complexity and vice versa).

4. Discussion

Interestingly, the empirical evidence presented in this paper suggests that the studied EBM process does not exhibit a clear link between energy consumption and part complexity. Using correlation coefficients, it has been demonstrated that shape complexity is only weakly related to energy consumption.

This observation can be contrasted with empirical data from machining processes. Morrow et al. [15] shows how consecutive CNC operations increase the energy invested into a part. As can be seen from Figure 7, the energy consumed by the various steps is highly non-uniform. This may be due to discrepancies in rough versus finish milling [15] or to variations in the specific energy consumption per unit of material removed [24]. The end result is the same: overall CNC energy consumption is the outcome of a sequence of manufacturing steps removing raw material and thereby manipulating raw material in plate form into a more complex final product.

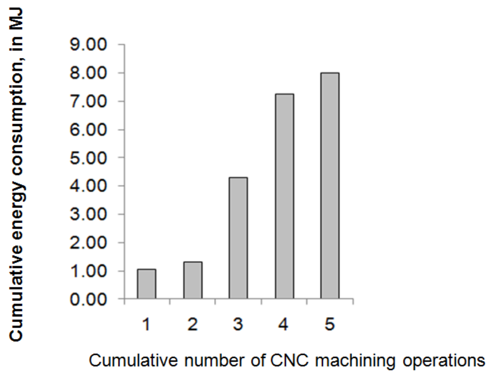

Figure 7: Cumulative energy consumption in MJ, by CNC operation
Image source: adapted from Morrow et al. [15]

As noted by Murr et al. [9], machining complex titanium parts from mill products is financially expensive. For titanium parts produced via CNC, there is thus a monetary cost incentive to keep deviation from the shape of the mill product to a minimum. However, in many part applications (transportation in particular), intricate and light weight components may enable significant cost and energy savings [25]. Therefore, manufacturing cost minimisation in CNC may be at odds with use-phase efficiency, both in terms of energy consumed during the part's use phase as well as in terms of operating cost.

5. Conclusions

The current paper has discussed EBM's ability to generate extra product shape complexity without increasing manufacturing energy requirements. It is shown that cross-sectional melting area can be viewed as the determinant of energy consumption per layer. As the amount of material deposited drives both cost and process energy consumption [19], this paper argues that cost minimisation is likely to inadvertently lead to virtuous knock-on effects: energy consumption is minimised during the manufacturing phase and, in weight sensitive applications, end-use efficiency may be improved. Such effects can be described as correctly aligning the private cost incentive with energy consumption reduction [26].

This is fundamentally different to CNC machining, where additional complexity is added in a sequence of discrete machining operations, resulting both in additional costs and waste streams. It should be noted that this analysis has not considered the energy embedded in the raw material. As CNC machining operations routinely result in significant waste streams in the form of machining swarf and EBM will result in little (if any) process related raw material wastage, a substantial additional energy saving may be available through the adoption of EBM.

Despite efforts to include environmental and social considerations in engineering decisions [27], private costs and benefits (accruing to individuals and organisations, as opposed to society) are normally viewed as the determinants of technology adoption decisions [28]. Thus, for the highly significant process innovation of AM, further research investigating commercial viability is needed. Moreover, it will be necessary to explore if the results presented in this paper can be generalised to other AM technology variants.

References

[1] Westkämper, E., Alting, L., and Arndt, G., Life Cycle Management and Assessment: Approaches and visions towards Sustainable Manufacturing (keynote paper), CIRP Annals – Manufacturing Technology, 49 (2), pp.501-526 (2000)

[2] Jovane, F., Yoshikawa, H., Alting, L., Boër, C. R., Westkämper, E., Williams, D., Tseng, M., Seliger, G., Paci, A. M., The incoming global technological and industrial revolution towards competitive sustainable manufacturing, CIRP Annals – Manufacturing Technology, 57 (2), pp. 641-659 (2008)

[3] Vijayaraghavan, A., Dornfeld, D., Automated energy monitoring of machine tools. CIRP Annals – Manufacturing Technology, 59 (1), pp.21-24 (2010)

[4] Levy, G. N., Schindel, R., Kruth, J. P., Rapid Manufacturing and Rapid Tooling with Layer Manufacturing (LM) Technologies, State of the Art and Future Perspectives, CIRP Annals – Manufacturing Technology, 52 (2), pp. 589-609 (2003)

[5] ASTM, ASTM F2792 - 12e1 Standard Terminology for Additive Manufacturing Technologies, [Online], Available from: www.astm.org/Standards/F2792.htm [Accessed: 04.10.2012] (2012)

[6] Arcam AB, Corporate website, [Online], available from: http://arcam.com [Accessed: 22.02.2013] (2013)

[7] Hopkinson, N., and Dickens, P. M., Emerging Rapid Manufacturing Processes. In N. Hopkinson, R. J. M. Hague, and P. M. Dickens, eds. Rapid Manufacturing – An Industrial Revolution for the Digital Age, Chichester: Wiley. Ch. 5. (2006)

[8] Heinl, P., Rottmair, A., Körner, C., and Singer, R. F., Cellular Titanium by Selective Electron Beam Melting. Advanced Engineering Materials, 9 (5), pp.360-364 (2007)

[9] Murr, L. E., Quinones, S. A., Gaytan, S. M., Lopez, M. I., Rodela, A., Martinez, E. Y., Hernandez, D. H., Martinez, E., Medina, F., Wicker, R. B., Microstructure and mechanical behaviour of Ti-6Al-4V produced by rapid-layer manufacturing, for biomedical applications. Journal of the mechanical behaviour of biomedical materials, 9 (1), pp.20-32 (2009)

[10] Frigola, P., Agustsson, R., Boucher, S., Murokh, A., Rosenzweig, J., Travish, G., Faillace, L., Cormier, D., Mahale, T. A, Novel fabrication technique for the production of RF photoinjectors, Proceedings of EPAC08, Genoa, Italy, pp. 751-753 (2008)

[11] Taminger, K. M. B., and Hafley, R. A., Characterization of 2219 Aluminium produced by electron beam freeform fabrication, Proceedings of the 13th Solid Freeform Fabrication Symposium, Austin, USA (2002)

[12] Strutt, P. R., A comparative study of electron beam and laser melting of M2 tool steel. Materials Science and Engineering, 44 (2), pp.239-250 (1980)

[13] Tuck, C. J., Hague, R. J. M., Ruffo, M., Ransley, M., and Adams, P.,. Rapid Manufacturing facilitated customization, International Journal of Computer Integrated Manufacturing, 21(3), pp.245-258 (2008)

[14] Ruffo, M., and Hague, R., Cost estimation for rapid manufacturing – simultaneous production of mixed components using laser sintering, Proceedings of IMech E Part B: Journal of Engineering Manufacture, 221(11), pp.1585-1591 (2007)

[15] Morrow, W. R., Qi, H., Kim, I., Mazumder, J., and Skerlos, S. J., Environmental aspects of laser-based and conventional tool and die manufacturing, Journal of Cleaner Production, 15(1), pp.932-943 (2007)

[16] Harrysson, O., Deaton, B., Bardin, J., West, H., Cansizoglu, O., Cormier, D., Marcellin-Little, D, Evaluation of titanium Implant Components Directly Fabricated Through Electron Beam Melting Technology, Proceedings of the Materials & Processes for Medical Devices Conference, Boston (2005)

[17] Åstebro, T., Sunk Costs and the Depth and Probability of Technology Adoption, The Journal of Industrial Economics, 52 (3), pp.381-399 (2004)

[18] Hague, R., Campbell, I., and Dickens, P., Implications on design of rapid manufacturing, Proceedings of IMechE Part C: Journal of Mechanical Engineering Science, Vol. 217, No. C1, 25-30 (2003)

[19] Baumers, M. Economic Aspects of Additive Manufacturing: Benefits, Costs and Energy Consumption, Ph.D. thesis, Loughborough University, United Kingdom (2012)

[20] Mognol, P., Lepicart, D., and Perry, N., Rapid prototyping: energy and environment in the spotlight. Rapid Prototyping Journal, 12(1), pp.26-34 (2006)

[21] Psarra, S., and Grajewski, T., Describing Shape and Shape Complexity Using Local Properties, Proceedings, 3rd International Space Syntax Symposium, Atlanta (2001)

[22] Baumers, M., Tuck, C., Wildman, R., Ashcroft, I., and Hague, R., Energy inputs to additive manufacturing: does capacity utilization matter? Proceedings of the Solid Freeform Fabrication (SFF) Symposium, The University of Texas at Austin, (2011).

[23] Le Bourhis, F., Kerbrat, O., Hascoet, J. Y., Mognol, P., Sustainable manufacturing: evaluation and modeling of environmental impacts in additive manufacturing, The International Journal of Advanced Manufacturing Technology, 69, 9-12, pp .1927-1939 (2013)

[24] Avram, O. I., and Xirouchakis, P., Evaluating the use phase energy requirements of a machine tool system, Journal of Cleaner Production, 19 (6-7), pp. 699-711 (2011)

[25] Helms, H., and Lambrecht, U., The Potential Contribution of Light-Weighting to Reduce Transport Energy Consumption, International Journal of Life Cycle Assessment, special issue, 12 (1) pp.58-64 (2007)

[26] Lovins, A. B., Negawatts – Twelve transitions, eight improvements and one distraction. Energy Policy, 24 (4), pp.331-343 (1996)

[27] Maxwell, D., and Van der Vorst, R., Developing sustainable products and services, Journal of Cleaner Production, 11 (8), pp.883-895 (2003)

[28] Stoneman, P., The economics of technological diffusion, 1st ed. Oxford: Blackwell (2002)